AD-A181 197 CRYSTAL GROWTH AND MECHANICAL PROPERTIES OF SEMICONDUCTOR ALLOYS(U) STANFORD UNIV CA DEPT OF MATERIALS SCIENCE AND ENGINEERING D A STEVENSON

1/1

UNCLASSIFIED 21 MAY 87 AFOSR-TR-87-0750 AFOSR-86-0158 F/G 9/1 NL

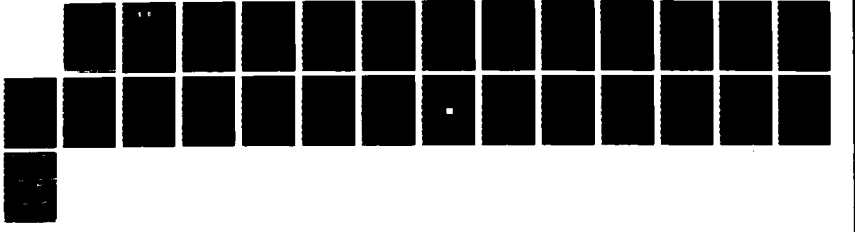

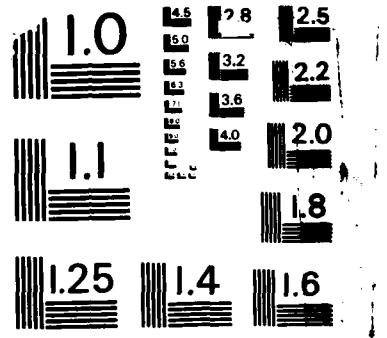

MICROCOPY RESOLUTION TEST CHART

NATIONAL BUREAU OF STANDARDS-1963-A

(2)

SECURITY CLASSIFICATION OF THIS PAGE

REPORT DOCUMENTATION P

1a. REPORT SECURITY CLASSIFICATION: UNCLASSIFIED	1b. RESTRICTI
2a. SECURITY CLASSIFICATION AUTHORI	3. DISTRIBUTI
2b. DECLASSIFICATION/DOWNGRADING SCHEDULE	Approved for Public Release Distribution Unlimited
4. PERFORMING ORGANIZATION REPORT NUMBER(S)	5. MONITORING ORGANIZATION REPORT NUMBER(S): AFOSR-TR- 87-0750
6a. NAME OF PERFORMING ORGANIZATION: Stanford University	6b. OFFICE SYMBOL (If applicable):
6c. ADDRESS (City, State and ZIP Code): Dept of Materials Science & Engineering, Stanford CA 94305	7a. NAME OF MONITORING ORGANIZATION: AFOSR
8a. NAME OF FUNDING/SPONSORING ORGANIZATION: AFOSR	8b. OFFICE SYMBOL (If applicable): NE
8c. ADDRESS (City, State and ZIP Code): Bldg 410, Bolling AFB DC 20332	7b. ADDRESS (City, State and ZIP Code): Bldg 410, Bolling AFB, DC 20332-6448
	9. PROCUREMENT INSTRUMENT IDENTIFICATION NUMBER: AFOSR-86-0158
	10. SOURCE OF FUNDING NOS.

PROGRAM ELEMENT NO.	PROJECT NO.	TASK NO.	WORK UNIT NO.
61102F	2306	B1	

11. TITLE (Include Security Classification): Crystal Growth and Mechanical Properties of Semiconductor Alloys

12. PERSONAL AUTHOR(S): Professor Stevenson

13a. TYPE OF REPORT	13b. TIME COVERED	14. DATE OF REPORT (Yr., Mo., Day)	15. PAGE COUNT
Annual Report	FROM 15/4/86 TO 14/4/87	87 May 21	23

16. SUPPLEMENTARY NOTATION

17. COSATI CODES			18. SUBJECT TERMS (Continue on reverse if necessary and identify by block number)
FIELD	GROUP	SUB. GR.	

19. ABSTRACT (Continue on reverse if necessary and identify by block number)

The mechanical properties of semiconductor materials are related to changes in electronic and optical properties that may occur during the processing of materials into wafers and wafers into devices. Recent theoretical models related hardness in ternary semiconductor alloys to fundamental atomic properties, but few datat are available. The report details the progress mad in exploring methods for mechanical property studies of these alloys. Three approaches were used: hardness measurements in thick films (10-100 micrometer) using conventional microhardness techniques; hardness measurements in thin films (less than 1 micrometer) using a nanoindenter; and the growth of bulk samples for use in conventional mechanical tests.

20. DISTRIBUTION/AVAILABILITY OF ABSTRACT	21. ABSTRACT SECURITY CLASSIFICATION
UNCLASSIFIED/UNLIMITED ☒ SAME AS RPT. ☐ DTIC USERS ☐	UNCLASSIFIED

22a. NAME OF RESPONSIBLE INDIVIDUAL	22b. TELEPHONE NUMBER (Include Area Code)	22c. OFFICE SYMBOL
Capt Malloy	(202) 767-4931	NE

DD FORM 1473, 83 APR EDITION OF 1 JAN 73 IS OBSOLETE.

SECURITY CLASSIFICATION OF THIS PAGE

AD-A181 197

Annual Report

for

April 15, 1986 - April 14, 1987

for

Contract AFOSR 86-0158
Project Task 2306/B1

Crystal Growth and Mechanical Properties of Semiconductor Alloys

Principal Investigator: D. A. Stevenson
Department of Materials Science and Engineering
Stanford University
Stanford, CA 94305

Sponsored by
Air Force Office of Scientific Research

Abstract

The mechanical properties of semiconductor materials are related to changes in electronic and optical properties that may occur during the processing of materials into wafers and wafers into devices. Recent theoretical models relate hardness in ternary semiconductor alloys to fundamental atomic properties, but few data are available. This report details the progress made in exploring methods for mechanical property studies of these alloys. Three approaches were used: hardness measurements in thick films (10-100 μm) using conventional microhardness techniques; hardness measurements in thin films (< 1 μm) using a nanoindenter; and the growth of bulk samples for use in conventional mechanical tests.

An isothermal vapor phase epitaxial method was used to grow oriented single crystal layers of $Hg_{1-x}Cd_xTe$ (x from 0.1 to 0.7) on CdTe substrates. The hardness values ranged from 33 kg/mm^2 to 69 kg/mm^2, which are comparable to hardness values in the literature obtained using individual bulk samples. Hardness measurements on bulk samples of $Zn_xCd_{1-x}Te$ (x from 0.0002 to 0.3) ranged from 49 kg/mm^2 to 102 kg/mm^2. Hardness measurements of two $Al_xGa_{1-x}As$ thin films (x=0.30 and 0.35) and undoped GaAs were made using the nanoindenter. The $Al_{0.3}Ga_{0.7}As$ film had higher hardness values than either the GaAs or the $Al_{0.35}Ga_{0.65}As$ film, which had surprisingly similar hardness values. Plastic indentation depths ranged from 49 nm to 241 nm, while hardness values ranged from 6.4 GPa to 8.2 GPa (650 kg/mm^2 to 830 kg/mm^2). A polycrystalline sample of $Ga_xIn_{1-x}Sb$ was grown using a vertical Bridgman technique. Hardness values are ~370 kg/mm^2, with a small decrease (7%) in the hardness as x values go from 0.9 to 0.7. Future work is described.

I. Introduction

The mechanical properties of semiconductor materials is a topic of practical and theoretical interest. The mechanical properties relate to the changes in electronic and optical properties that may accompany the processing of semiconductor materials into devices, particularly the introduction of dislocations upon thermal processing, slicing, polishing, ion implantation, and the application of films. Furthermore, the mechanical strength is of chief concern in the physical handling of wafers during processing and in the integrity of devices during service. Recent theoretical studies have related hardness in ternary semiconductor alloys to fundamental atomic properties, but comparison with experiments is limited because of insufficient information [1].

In spite of this obvious interest, there has been relatively little work done on this topic. A major reason is the difficulty in the preparation of bulk samples that are needed for conventional mechanical tests. There is usually a large separation between the liquidus and solidus on the pseudobinary phase diagrams of such systems, which leads to segregation during melt growth [2]. Even worse is the tendency in these systems for interface breakdown, due to constitutional supercooling, thus making crystal growth difficult [2-6].

The objective of this research program is to explore methods for determining the mechanical properties of ternary semiconductor alloy systems. To achieve this objective, we are initially exploring three possible approaches: hardness measurements on thick films (10-100μm) using conventional microhardness techniques; hardness measurements on thin films (< 1 μm) using a nanoindenter; and bend tests on bulk samples. In the first year, we have pursued these approaches with the following specific studies: $Hg_{1-x}Cd_xTe$ layers (x ranging from 0.1 to 0.7) were grown on CdTe substrates and microhardness measurements were made; microhardness measurements were made on bulk $Zn_xCd_{1-x}Te$ samples (x ranging from 0.0002 to 0.3); hardness measurements of AlGaAs and GaAs were made using a nanoindenter; and bulk growth, microprobe analysis, and microhardness

measurements of $Ga_xIn_{1-x}Sb$ were accomplished. Details of these activities are provided below.

II. Vickers Hardness Measurements

Since Vickers hardness measurements are made on both the thick epilayers and on bulk samples, we review some of the problems encountered in making the measurements. The Vickers hardness tester consists of a square based diamond pyramid that has an angle of 136° between opposite faces [7]. Weights of varying masses are used to apply the load, while a dashpot controls the loading rate. After the indentation is made, the diagonals of the indentation are measured at a magnification of 400. The diagonal lengths are then averaged and transformed into a hardness value.

There are several effects that must be considered in making hardness measurements: the effect of grain size; the differences in hardness in different grains and across twins; the photoplastic effect in certain semiconductors; and the effect of the anisotropy of crystals. The effect of grain size on hardness has been extensively studied in several commercially available metallic alloys (e.g., mild steels and brass). Hall (as cited in [7]) developed an equation for this relationship:

$$H = H_O + c\, L^{-1/2}$$

where H_O is the hardness of a single large grain, c is usually a constant, and L is the grain diameter. This increase in hardness with decreasing grain size arises from the pileup of dislocations at the grain boundaries. We believe that the ternary semiconductor alloys would behave similarly, but since all of our samples are either single crystals or large polycrystals, we are not concerned with this effect.

We have also investigated how hardness varies from grain to grain and across twins. Since different grains and twinned regions have different crystal orientations, we would expect changes in hardness as different slip systems are activated. Table I shows our results of Vickers hardness tests done on CdTe, In-doped CdTe, $Zn_{0.02}Cd_{0.98}Te$, and $Zn_{0.04}Cd_{0.96}Te$. The $Zn_{0.02}Cd_{0.98}Te$ and $Zn_{0.04}Cd_{0.96}Te$ samples show little

change in hardness either in different grains or twins; all the differences can be explained by experimental scatter. The CdTe and In-doped CdTe samples were etched with the Nakagawa etch (20 H_2O:20 H_2O_2:15 HF) to reveal crystal orientation. The region termed "twin #1" is oriented in the <111> direction, while the "twin #2" region is oriented 18.6° off the <100> direction. The CdTe and In-doped CdTe samples do show some differences in hardness across twins. The differences are not large (~10%), but they exhibit a pattern in that the regions in the <111> direction are harder than the regions 18.6° off the <100> direction in both sets of samples.

Another possible effect on the hardness of the II-VI ternary semiconductor alloys is the photoplastic effect (PPE). This photomechanical effect refers to a strong reversible increase or decrease in the flow stress of a sample (and therefore hardness) when the material is illuminated with photons of energy near the band gap. The photoplastic effect has been observed in CdS, ZnO, CdSe, CdTe, Si, and Ge [8-14]. Several models have been proposed to establish mechanisms for the PPE. Ahlquist and Carlsson [8, 9] proposed a pinning mechanism arising from the interaction between charged dislocations and oppositely charged native point defects, whose charges are changed by trapping photo-induced minority carriers. Gutmanas et al. [11,12] proposed a two-regime model depending on the magnitude of the applied shear stress, τ, with respect to the Peierls force, τ_p (the intrinsic lattice resistance arising from bonding directionality). When $\tau > \tau_p$, dislocation motion is controlled by interaction with local obstacles, whose structures are changed by light (e.g., charged point defects may trap photo-induced minority carriers). When $\tau < \tau_p$, dislocation motion is controlled by the nucleation of double kinks, whose formation energy is decreased by light. Nakagawa et al. [14,15] have proposed that the PPE is due to an increase in cross slip induced by electrical forces that arise from photo-induced charged point defects. Cole et al. [10] have proposed that any model of the PPE in HgCdTe must be based on some modification of the Peierls force that controls dislocation motion in HgCdTe.

Since illumination of a sample by the correct wavelength can increase flow stress and perhaps hardness by as much as 20%, we investigated the effect of normal laboratory lighting on Vickers hardness measurements. Table II shows our results in CdTe, $Zn_{0.04}Cd_{0.96}Te$, and $Hg_{0.2}Cd_{0.8}Te$ samples. The samples were illuminated with small incandescent spot lights (in addition to normal lab lighting) that increased the sample's temperature by no more than a couple of degrees. Normal laboratory lighting is fluorescent lighting with no added lamps. In the first CdTe sample, there appeared to be a small PPE (~5% increase in hardness), but the second sample showed no significant difference in hardness measurements taken in light or darkness. The first $Zn_{0.04}Cd_{0.96}Te$ sample also showed a very small increase in hardness (~2%) with illumination, while the second sample showed no significant differences. The $Hg_{0.2}Cd_{0.8}Te$ sample showed no photoplastic effect.

The last effect we investigated is the effect of crystal anisotropy on hardness. One may expect that the hardness may change if the sample is rotated, since different slip systems may be activated, as discussed with A. Sher [15]. Roberts [16] found that Knoop hardness measurements made on the (001) face of an InSb sample changed by as much as 20% at 20° C as the sample was rotated from 0° to 90° in 15° intervals. We investigated this effect by measuring the Vickers hardness of a (100) GaAs substrate and a (110) GaInSb sample as they were rotated in 15° intervals. As can be seen in Figure 1, there appears to be some change in hardness as a function of angle of rotation, but no clear pattern emerges.

Since Vickers hardness measurements were performed on both the thick epilayers and on bulk samples, we investigated the various problems encountered in making the measurements: the effect of grain size; the differences in hardness in different grains and twins; the photoplastic effect; and the effect of the anisotropy of crystals. We have found that all of these effects are either not applicable to our samples or are so small as to be negligible in making accurate hardness measurements.

III. Growth and Hardness Studies on $Hg_{1-x}Cd_xTe$ Epitaxial Layers

Thick films (5-20 μm) can be grown on a substrate using an isothermal vapor phase epitaxial (ISOVPE) method pioneered by Marfaing et al. [17]. An important new refinement of this method was made by Fleming [18], which was further developed in the present study to grow single crystal films of variable composition. There are two important advantages to this ISOVPE method: it is a relatively simple experimental technique and it produces an epilayer with a variation in composition. Thick films of $Hg_{1-x}Cd_xTe$ were grown on CdTe substrates. The method consists of placing a CdTe substrate in a vertical orientation with respect to a Te-rich HgTe source in an enclosed evacuated quartz ampule and annealing it at a constant temperature. Figure 2 shows a schematic diagram of the capsule. The resulting epilayer is quite thick (10-100 μm) and conventional microhardness measurements can be made. Futhermore, the composition varies in the epilayer and hardness can be determined as a function of composition for an oriented single crystal layer. Figure 3 shows hardness values as a function of the values of x in the $Hg_{1-x}Cd_xTe$ epilayers ranging from 0.1 to 0.7. The hardness values range from 33 kg/mm^2 to 69 kg/mm^2, which are comparable to hardness values determined by Cole et al. [10], who used individual bulk specimens grown by the Bridgman method. Figure 4 shows how our data compare with the data of Cole et al., Kurilo et al., Sharma et al., and Koman and Pashovskii [10]. Although there is some scatter in our data at higher x values, they are in agreement with Cole's data. Our method is an efficient way to survey a broad range of composition on a single oriented epilayer rather than measuring separately prepared samples of different orientation.

It is possible that the ISOVPE method can be used for systems other than HgTe and CdTe [17,19]. The limitations are the lattice mismatch and the relative vapor pressures of the components. Possible semiconductor systems that may be grown by this method are: ZnTe-HgTe; ZnTe-CdTe; HgTe-PbTe; HgTe-GeTe; GeTe-PbTe; GaP-InP; GaAs-InAs; GaP-GaAs; and InP-InAs. Table III lists the lattice mismatch and melting temperatures for

the candidate systems. The systems with the smaller lattice mismatch should produce epilayers of higher quality than those with larger lattice mismatch. We will explore this method with the most promising of these systems and, if good quality films of sufficient thickness can be grown, microhardness measurements will be made as a function of composition.

IV. Vickers Hardness of $Zn_xCd_{1-x}Te$

We investigated the hardness of $Zn_xCd_{1-x}Te$ to see if it exhibits the nonlinear hardness behavior seen in HgCdTe. Our samples included CdTe and $Zn_xCd_{1-x}Te$ samples with x values ranging from 0.0002 to 0.3. The samples were bulk crystals grown by the Bridgman technique here at Stanford. Figure 5 shows the Vickers hardness as a function of the x value of $Zn_xCd_{1-x}Te$. Hardness values range from 49 kg/mm^2 to 102 kg/mm^2.

This strengthening effect is in agreement with the theoretical predictions of Sher et al. [20]. They predict that the hardness of tetrahedrally bonded semiconductors is a strong function of the reciprocal of the bond length. When ZnTe (with a bond length of 2.643 Å) is added to CdTe (with a bond length of 2.805 Å), the alloyed ternary semiconductor has a shorter bond length than pure CdTe. This should result in an increase in hardness, which is seen in our data. Qadri et al. [21] have published compression data that indicate that $Zn_{0.04}Cd_{0.96}Te$ is about 2% stiffer than CdTe. Our hardness data indicate that the strengthening effect (as evidenced by the Vickers hardness) is much more than 2%. We are presently exploring the growth of $Zn_xCd_{1-x}Te$ samples at higher values of x using the close spaced vapor transport method to extend the hardness versus composition curve.

V. Nanoindenter Studies

Most films prepared by MBE or MOCVD are < 0.1 μm and conventional microhardness measurements cannot be made on such thin films. A new instrument, the nanoindenter, shows promise for obtaining meaningful measurements on such films. The nanoindenter has several potential advantages: hardness can be obtained over a small area and on very thin films; indentation imaging is not needed; and hardness can be monitored

continuously with depth. Important capabilities of the nanoindenter include a minimum indentation depth of 200 Å; force resolution of 0.5 μN; displacement resolution of 2 Å; and a typical indentation rate of 30 Å/sec [22].

Three samples were tested in the past year using the nanoindenter: a (100) undoped GaAs wafer and two $Al_xGa_{1-x}As$ films, deposited on GaAs by MBE, with thicknesses of ~3000 Å and compositions of x=0.30 and 0.35. The AlGaAs samples were provided by Dr. Martin P. Scott of Hewlett Packard.

Figure 6 shows the hardness as a function of effective depth (i.e., plastic depth) of the indentation from the three samples. The effective depth values range from 49 nm to 241 nm and the hardness values range from 6.4 GPa to 8.2 GPa (650 kg/mm^2 to 830 kg/mm^2). The hardness of the GaAs and the $Al_{0.35}Ga_{0.65}As$ samples increased 20% and 22%, respectively, as the effective depths went from 67 nm to 241 nm. The hardness of the $Al_{0.3}Ga_{0.7}As$ sample increased only 5% as the effective depths went from 49 nm to 241 nm. The $Al_{0.3}Ga_{0.7}As$ film shows higher hardness values than either the GaAs substrate or the $Al_{0.35}Ga_{0.65}As$ film; however, the hardness values changed only slightly with composition. A literature search revealed only two papers reporting the hardness of AlAs or AlGaAs. Borshchevskii and Tretiakov [23] found the Vickers hardness of AlAs to be 505 kg/mm^2. Swaminathan et al. [24] reported the Knoop hardness of n-type $Al_xGa_{1-x}As$ (x=0.057-0.079) to be 669 kg/mm^2 as compared to 640 kg/mm^2 for n-type GaAs and that of p-type $Al_xGa_{1-x}As$ (x=0.057-0.079) to be 601 kg/mm^2 as compared to 598 kg/mm^2 for p-type GaAs. From these data, we conclude that the AlGaAs films should be slightly harder than GaAs. The very small differences between the hardness values of the GaAs substrate and the $Al_{0.35}Ga_{0.65}As$ film may arise from an unexpected influence of the GaAs substrate or the hardness values may be a maximum close to x values of 0.30 and trending towards even lower values.

Doerner et al. [25] have found a thickness effect on the strength of Al and W thin films deposited on Si substrates. The hardness of the Al films increased for decreasing

film thickness, while the hardness of the W films decreased for decreasing film thickness. They suggest that dislocations generated in the interior of the film are repelled from the interface when the substrate is elastically stiffer than the film (as for the Al film), while they are attracted to the interface when the substrate is more compliant than the film (as for the W film).

Future work will include: measuring the hardness of more $Al_xGa_{1-x}As$ films at different values of x to answer the above questions; measuring the hardness of $In_{1-x}Ga_xAs$ thin films to compare with the predictions of A. Sher; and investigating the influence of the substrate on the hardness of the films for different film thicknesses.

VI. Bulk Crystal Growth of $Ga_xIn_{1-x}Sb$

The pseudobinary semiconductor, $Ga_xIn_{1-x}Sb$, was chosen for bulk growth because the melting temperature is fairly low and because there is considerable literature on the growth of this system arising from an interest in its use for Gunn devices and three-level oscillators [26]. Single crystal growth of $Ga_xIn_{1-x}Sb$ is difficult because of the high segregation of GaSb in InSb, interface breakdown due to constitutional supercooling, and low diffusion rates in the material [27]; however, we expect to obtain coarse grained samples of varying composition suitable for microhardness measurements.

A bulk sample was grown by a vertical Bridgman technique using an encapsulated crucible. The liquid was homogenized by a five day anneal and growth was made at an 0.8 mm/day rate. The ingot was then removed and sectioned. Micrographs of polished and etched longitudinal and transverse sections are shown in the seven month progress report submitted in November 1986.

Microprobe analysis was performed on the ingot, giving the composition profile seen in Figure 7. The sudden change in composition was the result of a premature termination of the crystal growth which was required to accomplish hood repairs. The quenched section of the ingot consists of very small grains (1 mm), while the region of slow growth has quite large grains (some as long as 20 mm). Figure 8 shows Vickers

hardness as a function of composition. The hardness values are approximately 370 kg/mm^2 with a ~7% decrease in hardness as the x values go from 0.9 to 0.7.

Another Bridgman crystal growth at a lower value of x (nominally, x=0 3) is in progress. We will also investigate two additional techniques for obtaining single crystals: stress annealing [28]; and solid state recrystallization [29]. If sufficiently large samples can be made, other mechanical tests, such as bend tests and impact tests, will be explored. In addition, we will confer with other investigators regarding the determination of the elastic constants for these alloys.

VII. Summary

The research activity for the first year of our study of the mechanical properties of ternary semiconductor alloys has been described. We report progress in three areas: thin films; thick films; and bulk samples. Conventional microhardness measurements were made on oriented single crystal layers of $Hg_{1-x}Cd_xTe$, with values of x ranging from 0.1 to 0.7. The hardness values ranged from 33 kg/mm^2 to 69 kg/mm^2 and were comparable to those reported by Cole et al. [10], who used individual bulk crystals of unknown orientation. Vickers hardness measurements were also made on $Zn_xCd_{1-x}Te$ samples with x values ranging from 0.0002 to 0.3 and hardness values ranging from 49 kg/mm^2 to 102 kg/mm^2. An increase in hardness supports Sher's theory of bond strengthening. Hardness measurements were made on two thin films of $Al_xGa_{1-x}As$ (x=0.30 and 0.35) and a (100) undoped GaAs wafer. The measured hardness of the $Al_{0.3}Ga_{0.7}As$ film was only slightly higher than either the GaAs substrate or the $Al_{0.35}Ga_{0.65}As$ film, which have similar hardness values. There is a surprisingly small change in hardness with composition in this system, which is still being analyzed. A bulk crystal of $Ga_xIn_{1-x}Sb$ was grown using a vertical Bridgman technique and microhardness measurements and microprobe analysis were done. The hardness values averaged 370 kg/mm^2 with a small decrease (~7%) as the x values went from 0.9 to 0.7.

Work continues in each of the three areas of study. The ISOVPE method will be explored in other semiconductor systems (e.g., ZnTe-HgTe, GaP-InP) and, if good quality films of sufficient thickness can be grown, microhardness measurements as a function of composition will be made. The hardness of $Al_xGa_{1-x}As$ thin films of varying x values will be measured to answer the questions mentioned previously. If samples can be obtained, the hardness of $In_{1-x}Ga_xAs$ thin films will also be measured to provide an experimental basis for A. Sher's theoretical model. Two techniques to produce grain coarsening, stress annealing and solid state recrystallization, will be studied using $Ga_xIn_{1-x}Sb$ bulk samples.

There are exciting questions and trends arising as this research progresses. Both $Zn_xCd_{1-x}Te$ and $Hg_{1-x}Cd_xTe$ ternary alloy systems show substantial hardness increase above a simple linear law (at least at the lower values of x). This implies a substantial "alloy hardening effect" in these pseudobinary systems. Will there be similar trends in other pseudobinary systems, for example, in the AlAs-GaAs system? There are also questions of substrate effects and interface strain on the film hardness values. How significant are substrate effects on the measured microhardness and are these factors important only near the film-substrate interface? A related question concerns the difference in hardness of strained layer superlattices (such as Si-Ge) and the corresponding homogeneous alloy.

References

(1) A. Sher, A. Chen, W. E. Spicer, and C. Shih, "Proceedings of the 1984 U.S. Workshop on the Physics and Chemistry of Mercury Cadmium Telluride: American Vacuum Society and American Institute of Physics (1985)", T. Casselman, editor.

(2) M. C. Flemings, "Solidification Processing" McGraw Hill (1973), p. 64.

(3) W. W. Mullins and R. F. Sekerka, J. Appl. Phys., 34:323 (1963); 35:444 (1964).

(4) R. F. Sekerka, J. Appl. Phys., 36:264 (1965).

(5) R. F. Sekerka, J. Phys. Chem. Solids, 28:983 (1967).

(6) R. F. Sekerka, J. Crystal Growth, 3:71 (1968).

(7) D. Tabor, "Proceedings of the Institute of Physics, F, Physics in Technology," 1:145 (1970).

(8) C. N. Ahlquist, M. J. Carrol, and P. Stroempl, J. Phys. Chem. Solids, 33: 337 (1972).

(9) L. Carlsson and C. N. Ahlquist, J. Appl. Phys., 43:2529 (1972).

(10) S. Cole, M. Brown, and A. F. W. Willoughby, J. Mat. Sci., 17:2061 (1982); 20:274 (1985).

(11) E. Y. Gutmanas and P. Haasen, Journal de Physique, 40:C6-169 (1979).

(12) E. Y. Gutmanas, N. Travitzky, and P. Haasen, Phys. Stat. Sol. (a), 51: 435 (1979).

(13) K. H. Kusters and H. Alexander, Physica 116B:594 (1983).

(14) K. Nakagawa, K. Maeda, and S. Takeuchi, J. Phys. Soc. Jap. 49:1909 (1980); 50:3040 (1981).

(15) A. Sher, Stanford Research Institute, personal communication.

(16) S. G. Roberts, Phil. Mag. A 54:37 (1986).

(17) Y. Marfaing, G. Cohen-Solal, and F. Bailly, "Proceedings of an International Conference on Crystal Growth, Boston, 20-24 June 1966," H. S. Peiser, editor.

(18) J. G. Fleming, "Growth and Properties of Mercury Cadmium Telluride Investigated Using Isothermal Techniques," Ph.D. dissertation, Stanford University, September 1986.

(19) M. H. Kalisher, Santa Barbara Research Center, personal communication.

(20) A. Sher, A. B. Chen, and W. E. Spicer, Appl. Phys. Lett. 46:54 (1985).

(21) S. B. Qadri, E. F. Skelton, A. W. Webb, and J. Kennedy, Appl. Phys. Lett. 46:257 (1985).

(22) M. F. Doerner and W. D. Nix, J. Mater. Res. 1:601 (1986).

(23) A. S. Borshchevskii and D. N. Tretiakov (1962) as cited in "Semiconductors and Semimetals" 4:12 (1968).

(24) V. Swaninathan, W. R. Wagner, and P. J. Anthony, J. Electrochem. Soc. 130:2468 (1983).

(25) M. F. Doerner, D. S. Gardner, and W. D. Nix, J. Mater. Res. 1:845 (1986).

(26) A. Joullie, P. Esquirol, and G. Bougnot, Mat. Res. Bull. 9:641 (1974).

(27) A. Joullie, J. Allegre, and G. Bougnot, Mat. Res. Bull. 7:1101 (1972).

(28) S. Sen, W. R. Wilcox, and R. A. Lefever, Met. Trans. A 9A:462 (1978).

(29) W. F. H. Micklethwaite, in "Semiconductors and Semimetals," 18:47 (1981).

(30) CRC Handbook of Chemistry and Physics, 61st edition (1980-1981).

TABLE I. The Effect of Grains and Twins on Vickers Hardness

Sample	Grain or Twin	Vickers Hardness (kg/mm^2)
$Zn_{0.02}Cd_{0.98}Te$	twin #1	55.7 (2.0)*
	twin #2	56.9 (1.3)
	grain #1	54.8 (3.5)
	grain #2	54.4 (2.7)
$Zn_{0.04}Cd_{0.96}Te$	grain #1	60.7 (1.4)
	grain #2	60.3 (0.9)
CdTe sample #1	twin #1	48.4 (2.1)
	twin #2	44.4 (1.0)
CdTe sample #2	twin #1	47.0 (0.8)
	twin #2	42.3 (1.0)
In-doped CdTe #1	twin #1	50.0 (1.6)
	twin #2	44.7 (0.8)
In-doped CdTe #2	twin #1	49.3 (1.1)
	twin #2	43.3 (0.6)

* The standard deviation of the data is in parenthesis.

TABLE II. The Effect of Lighting on Vickers Hardness

Sample	Lighting	Vickers Hardness (kg/mm^2)
CdTe sample #1	normal lab	50.3 (0.5)*
	lamps at lowest setting[1]	53.0 (0.2)
	lamps at medium setting	53.0 (0.4)
	lamps at highest setting	53.3 (0.7)
CdTe sample #2	normal lab	50.0 (1.4)
	darkness	49.2 (0.7)
$Zn_{0.04}Cd_{0.96}Te$	normal lab	63.4 (0.1)
sample #1	lamps at medium setting	65.3 (0.9)
$Zn_{0.04}Cd_{0.96}Te$	normal lab	61.1 (1.5)
sample #2	lamps at highest setting	59.5 (0.9)
	darkness	60.7 (1.1)
$Hg_{0.8}Cd_{0.2}Te$	normal	34.6 (0.7)
	darkness	33.5 (0.7)

* The standard deviation of the data is in parenthesis.

[1] The lamps are 10^{-3} watts/cm^2 at the highest setting.

Table III. Lattice Mismatch and Melting Temperatures of Selected II-VI and III-V Systems

System	% Lattice Mismatch	Melting Temperatures (K)
ZnTe-HgTe	5.3	ZnTe 1568 HgTe 943
ZnTe-CdTe	6.1	ZnTe 1568 CdTe 1365
HgTe-PbTe	0.3	HgTe 943 PbTe 1180
HgTe-GeTe	7.1	HgTe 943 GeTe 998
GeTe-PbTe	7.4	GeTe 998 PbTe 1180
GaP-InP	7.4	GaP 1750 InP 1330
GaAs-InAs	7.0	GaAs 1510 InAs 1215
GaP-GaAs	3.7	GaP 1750 GaAs 1510
InP-InAs	3.2	InP 1330 InAs 1215

(Lattice parameters and melting temperatures from [17, 30])

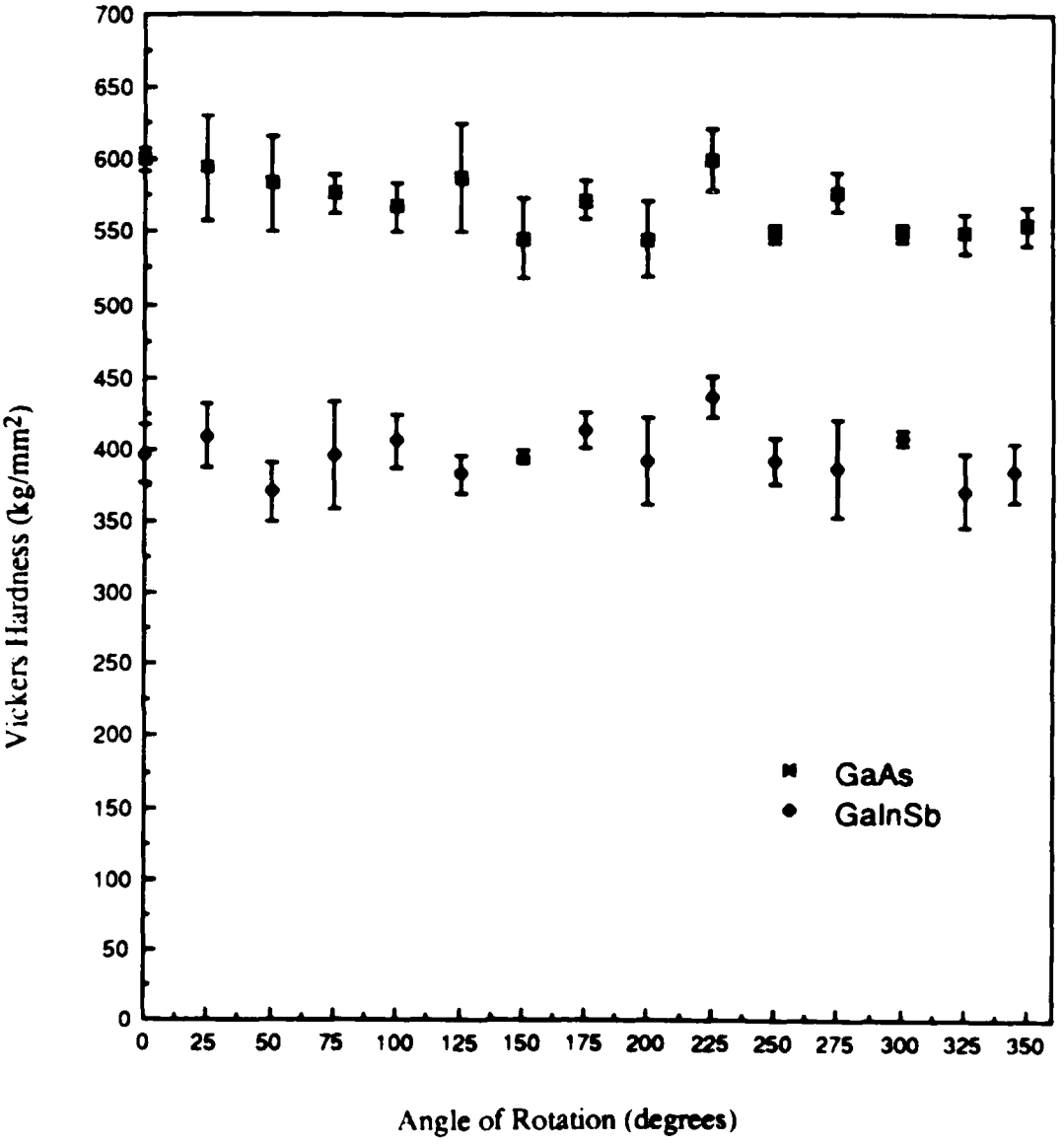

Figure 1. The effect of the angle of rotation on Vickers hardness on a (100) GaAs substrate and a (110) $Ga_{0.8}In_{0.2}Sb$ ingot. Error bars are ± one standard deviation.

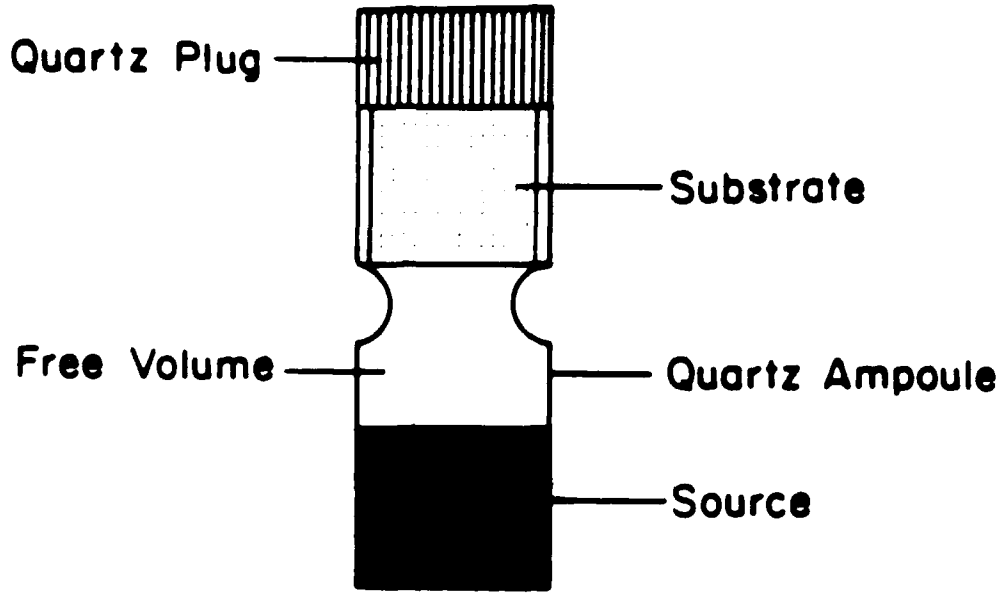

Figure 2. The geometry used in the ISOVPE experiments. Different points on the substrate are different distances from the source, which causes a gradient in composition.

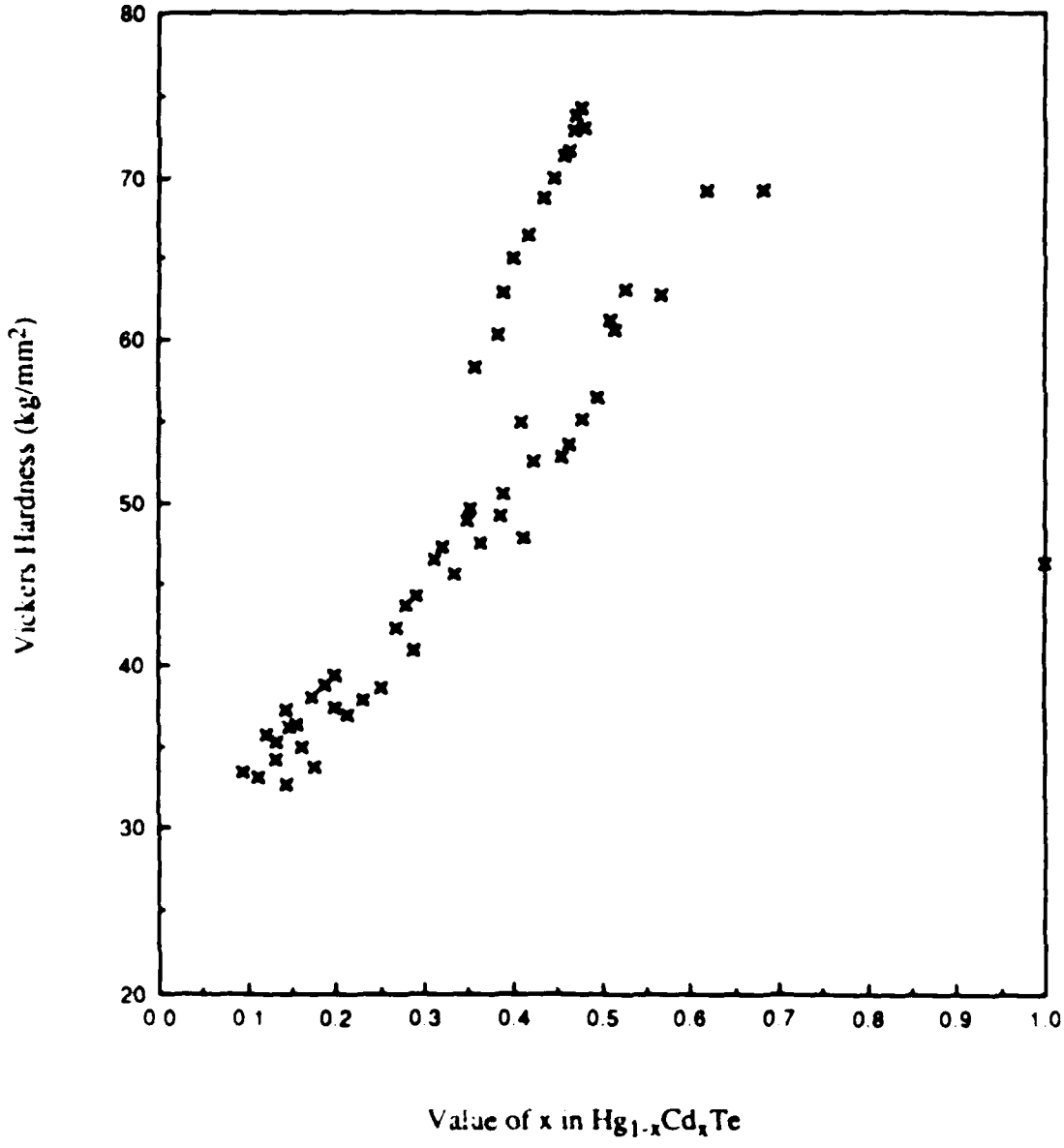

Figure 3. The Vickers hardness plotted as a function of composition in $Hg_{1-x}Cd_xTe$.

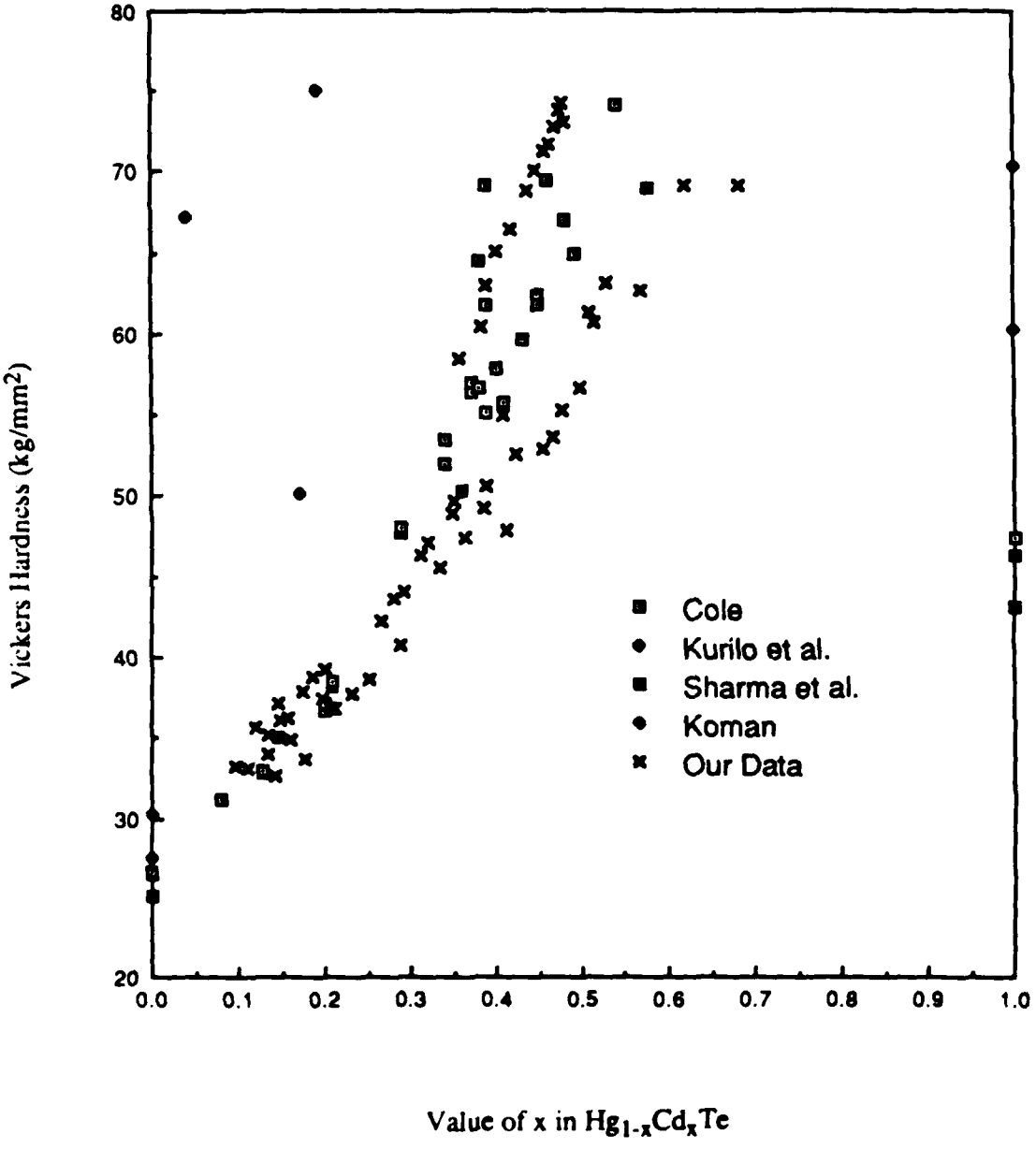

Figure 4. Our data of Vickers hardness plotted as a function of composition in $Hg_{1-x}Cd_xTe$ as compared with those of Cole, Kurilo et al., Sharma et al., and Koman and Pashovskii (as cited in [10]).

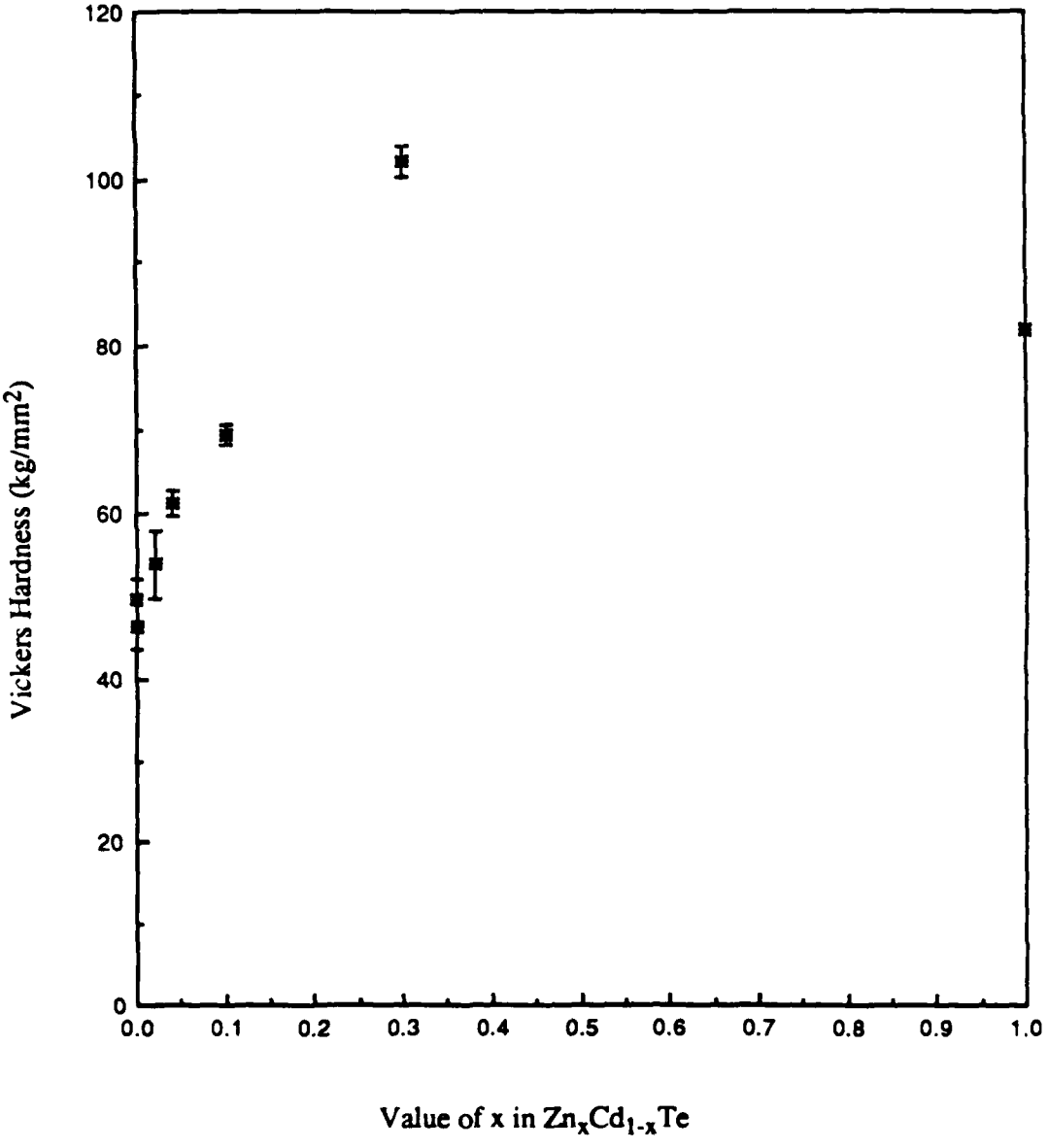

Figure 5. The Vickers hardness plotted as a function of composition of bulk $Zn_xCd_{1-x}Te$ samples.

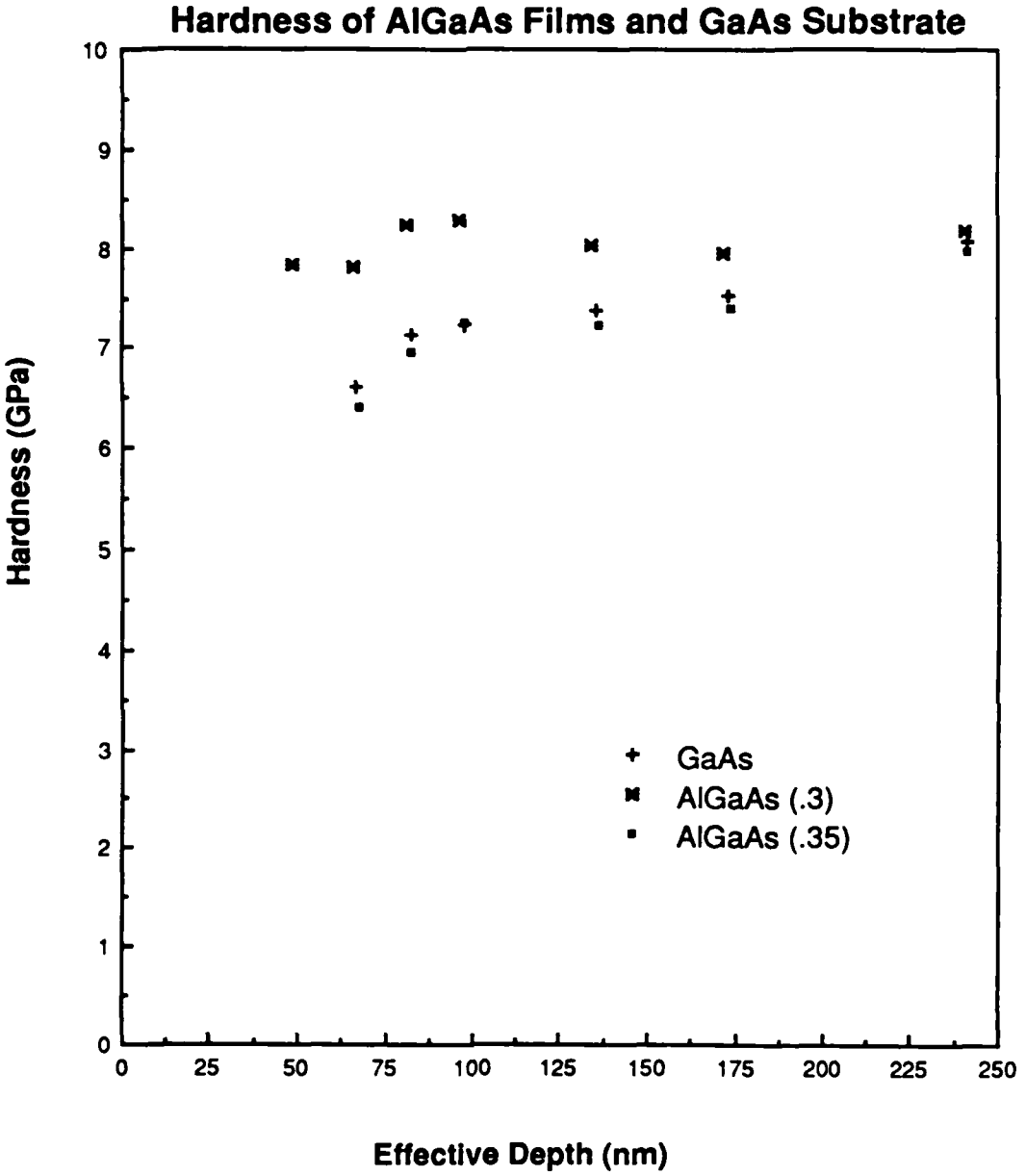

Figure 6. The hardness of a (100) GaAs substrate and two thin films of $Al_xGa_{1-x}As$ (x=0.3 and 0.35) plotted as a function of effective depths. The films were deposited on GaAs substrate by MBE and are ~3000 Å thick.

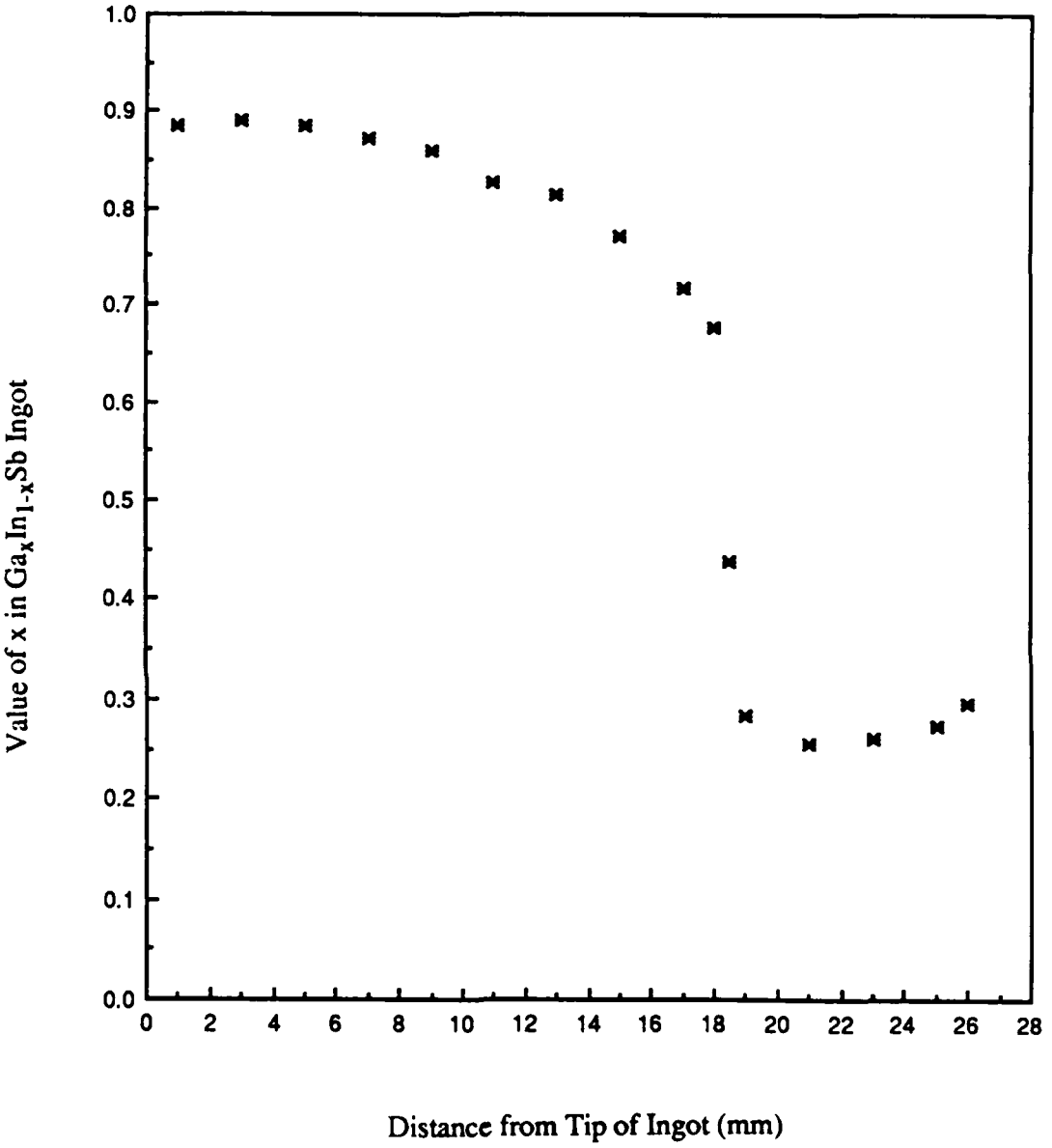

Figure 7. The value of x in a $Ga_xIn_{1-x}Sb$ ingot plotted as a function a distance from the tip of the ingot. The composition was measured by microprobe analysis.

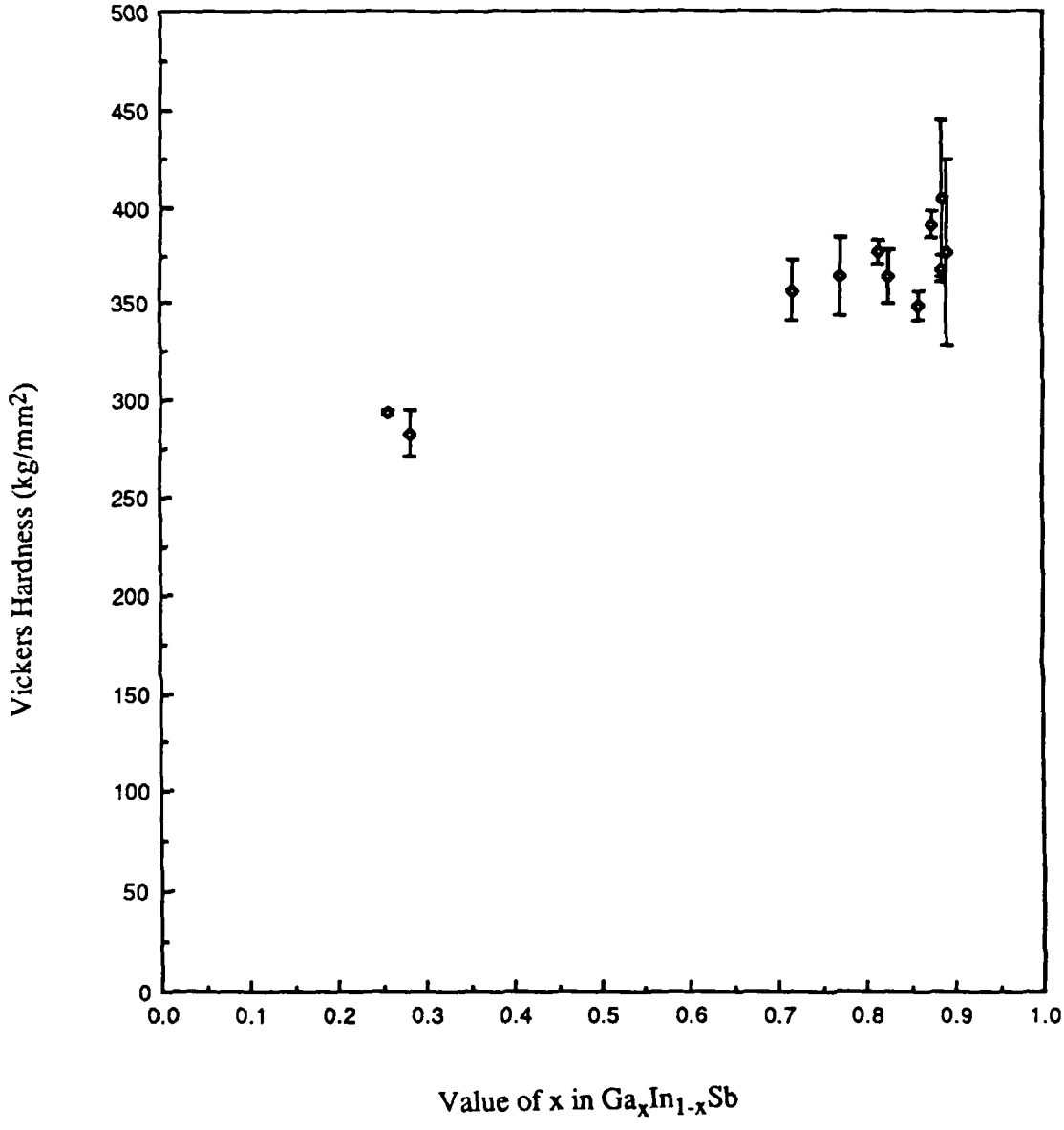

Figure 8. The Vickers hardness plotted as a function of composition in a $Ga_xIn_{1-x}Sb$ ingot.

END

7-87

DTIC